Solution Structure of Amyloid β-Peptide (25−35) in Different Media

Anna M. D'Ursi,[§] Maria R. Armenante,[§] Remo Guerrini,[†] Severo Salvadori,[†] Giuseppe Sorrentino,[#] and Delia Picone*[,‡]

Dipartimento di Scienze Farmaceutiche, Università di Salerno, Via Ponte Don Melillo 11c, 84084 Fisciano, Italy, Dipartimento di Scienze Farmaceutiche, Università di Ferrara, Via Fossato di Mortara 17-19, 44100 Ferrara, Italy, Università degli Studi di Napoli "Parthenope", Via Acton 38, 80133 Napoli, Italy, and Dipartimento di Chimica, Università degli Studi di Napoli "Federico II", Via Cintia 26, Complesso Universitario di Monte S. Angelo, 80126 Napoli, Italy

Received January 16, 2004

The design of molecules able to interact with the amyloid peptides either as inhibitors of fibril formation or as inhibitors of amyloid membrane pore formation represents one of the most relevant approaches in the development of anti-Alzheimer therapies. Aβ-(25−35), sequence GSNKGAIIGLM, is a highly toxic synthetic derivative of amyloid β-peptides (Aβ-peptides), which forms fibrillary aggregates. Here, we report the NMR and CD investigation of Aβ-(25−35) in a membrane-mimicking environment and in isotropic mixtures of water and fluoroalcohols to scan its conformational properties as a function of the medium. The analysis of the 3D structures in the mentioned conditions indicates a propensity of the peptide to behave as a typical transmembrane helix in the lipidic environment. In media characterized by different polarity, it loses the structural regularity at specific points of the sequence as a function of the environment. Furthermore, a comparison with the solution structure of full-length amyloid peptides suggests a role for the 25−27 kink region, which appears to be a general feature of all peptides under the solution conditions explored.

Introduction

Alzheimer's disease (AD) is a member of a heterogeneous family of diseases referred to as amyloidosis, characterized by deposits of amyloid in a variety of organs.[1,2] At present, almost 20 human diseases associated with the presence of insoluble aggregates of normally soluble proteins resulting in the formation of extracellular deposits have been identified.[3] Through self-assembly these proteins produce regular fibrillary structures possessing a predominant β-sheet conformation.[4] The amyloid deposits are the major constituent of the extracellular senile, or neuritic, plaques characteristic of brain tissue affected by AD. The primary proteinaceous component of neuritic plaques is a peptide composed of 39−42 amino acid residues[5] and referred to as amyloid β-peptide (Aβ). The Aβ molecules are derived from a type I transmembrane protein containing 695−770 amino acids, known as Aβ precursor protein (APP), by the action of the β- and γ-secretases.[6] Aβ-(1−42) is the most prone to aggregation and is produced in larger quantities in familial forms of AD.

Although a large consensus exists about the central role of Aβ in AD, the biophysical and biological mechanisms that underlie its toxicity are still controversial. A great deal of evidence supports the hypothesis that Aβ fibrillogenesis is a seminal pathogenetic event in AD.[7] It is natural to think that plaques adjacent to the membrane can damage it or even that the mechanical blockage by plaques of cellular exchanges with the outer environment can lead to the cellular death.[8] However, still problematic, as argued by Terry,[9] is the weak correlation between fibrillary amyloid load and measures of neurological dysfunction. Recent studies on Aβ support the possibility that nonfibrillary oligomeric species are pathogenic.[10,11] These data have led to the hypothesis that the Aβ neurotoxicity is related to different processes of membrane interaction and destabilization culminating in membrane pore formation and disruption. This hypothesis is supported also by the surprising similarity of the structure of Aβ-(1−42) recently solved in our lab[12] to the fusion domain of influenza hemagglutinin in an apolar environment. According to this hypothesis, the α-helical peptide would induce formation of membrane channels, allowing the penetration of substances that can cause neuronal death. The ability of Aβ to induce vesicle fusion and the recent observation that it can enhance infection at the stage of attachment or entry into the cell of several viruses[13] further support this hypothesis. Whatever the pathogenic mechanism of the AD would be, the conformational behavior of soluble forms of Aβ appears to play a critical role. Although Aβ peptides were identified several years ago, still relatively few structural studies describe the conformation of these molecules in their soluble or aggregated forms. Structural studies of these peptides are indeed strongly hampered by the low solubility in water and by their tendency to aggregate. In the search for the conditions that overcome these limitations, the most interesting datum is that Aβ peptides are crucially affected by the environmental conditions. Consistently the study of the conformational preferences of these peptides in different media appears to be crucial for shedding light on their intrinsic structural properties related to the Aβ fibril formation or to membrane disruption activity.

* To whom correspondence should be addressed. Phone: +39-081-674406. Fax: +39-081-674409. E-mail: picone@unina.it.
[§] Università di Salerno.
[†] Università di Ferrara.
[#] Università degli Studi di Napoli "Parthenope".
[‡] Università degli Studi di Napoli "Federico II".

10.1021/jm040773o CCC: $27.50 © 2004 American Chemical Society
Published on Web 07/21/2004

It has been proposed that Aβ-(25−35) represents the biologically active region of Aβ because it represents the shortest fragment that exhibits large β-sheet aggregated structures and retains the toxicity of the full-length peptide.[14] Several reports have also indicated that Aβ-(25−35), in a manner similar to that of Aβ-(1−42), undergoes a conformational transition from a soluble, random-coil form to aggregated fibrillary β-sheet structures, depending on the environmental conditions.[15] A more detailed conformational study performed by 2D NMR in LiDS micelles, pH 4.0, has indicated the presence of a well-ordered α-helical stretch encompassing residues 28−34.[16] Furthermore, CD and Fourier transform infrared spectroscopy have shown that upon addition of lipid vesicles containing negatively charged lipids the equilibrium shifts almost completely toward β-sheet structure formation.[15,17] Because of these properties Aβ-(25−35) has been often chosen as a model for full-length Aβ in structural and functional studies.

We describe here the conformational analysis by CD and NMR spectroscopies of Aβ-(25−35) in different experimental conditions to evaluate the structural properties of the Aβ segment in a membrane-mimicking environment and in isotropic media with different polarity. Micellar solutions of SDS are widely used to test the structural behavior of biomolecules known to interact with cellular membrane. The NMR study of Aβ-(25−35) in SDS in the presence of spin labels allowed us to investigate the structural behavior of the peptide in a lipid environment and to establish the orientation of the peptide with respect to the membrane. In addition, we have performed a structural investigation by CD and 2D NMR spectroscopy in water/fluorinated alcohol mixtures. These mixtures have been reported as helical stabilizing agents[18] and are also able to dissolve fibrillar aggregates of Aβ-(1−40).[19] To scan the conformational characteristics of this peptide in different polarity conditions, we collected data moving from a basically aqueous medium of water/HFIP, 80/20 v/v, to a basically apolar water/HFIP, 20/80 v/v. Although this shorter fragment does not give rise to aggregates, a conformational transition leading to a drastic reduction of the folded ordered structure is observable.

The study of the Aβ-(25−35) in the mentioned conditions could open the way to the design and the synthesis of molecules able to antagonize the membrane pore formation activity of Aβ peptides. Alternatively the detailed description of the conformational transition is a key step for designing aggregation inhibitors. Last but not least it seems very exciting the possibility that peptides designed from Aβ can be used to enhance the viral cell permeation[13] and may be useful for setting up a gene delivery therapy based on retroviral vectors.

Results

1. SDS Analysis. 1.1. NMR Spectrometry. A whole set of 1D and 2D proton spectra were recorded in aqueous solution of 100 mM SDS, pH 4.15. To check the absence of aggregation, spectra were acquired in the concentration range of 0.5−15 mM. No significant changes were observed in the distribution and in the shape of the ^{1}H resonances, indicating that no aggregation phenomena occurred in this concentration range. Complete assignment of the proton spectra of Aβ-(25−35) was achieved according to the Wüthrich procedure[20] via the usual systematic application of DQF-COSY, TOCSY, and NOESY experiments[21−23] with the support of the SPARKY software package.[24] The analysis of the NOE pattern revealed the presence of the typical helical (i, i + 2) and (i, i + 3) medium range connectivities encompassing the C-terminal residues, whereas less regularity was detected in the N-terminal segment, characterized by the prevalence of more disordered structures. In particular αN(i, i + 2) involves the residues Gly 29-Ile 31, Ile 31-Gly 33, and Ile 32-Leu 34, whereas αN(i, i + 3) connectivity involves the residues Ile 32-Met 35.

The structure calculation by means of DYANA software[25] and based on the NOE-derived interprotonic distances as restraints confirmed the previous structural results in LiDS.[16] In the SDS micelles environment, Aβ-(25−35) is characterized by a well-ordered α-helical structure involving the residues 28−34. The rmsd for the backbone between residues 28−34 and 25−27 are respectively 0.56 and 1.27 Å.

1.2. Spin-Label Studies. The NMR analysis in SDS was the starting point to investigate the positioning of the peptide with respect to the surface and interior of the micelle, using 5-doxylstearic acid and 16-doxylstearic acid as paramagnetic probes. Both compounds contain a doxyl headgroup, a cyclic nitroxide with unpaired electron, that is bound to the aliphatic chain carbon in position 5 or 16, respectively. Unpaired electrons lead to dramatically accelerated longitudinal and transverse relaxation rates of protons in spatial proximity via highly efficient spin−electron relaxation. It has been shown that these paramagnetic probes are able to induce broadening of the NMR signals or a decrease of resonance intensities for residues close to the surface (5-doxyl) or deeply buried in the micelle (16-doxyl), respectively.[26,27] TOCSY spectra of Aβ-(25−35) either in the presence or in the absence of the spin labels, keeping constant all other conditions, were compared. All signal intensities remained constant upon addition of 5-doxylstearic acid, thereby proving that no residue of Aβ-(25−35) interacts with the micelle surface (data not shown). In Figure 1 a comparison of the Hα-NH region of TOCSY spectra of Aβ-(25−35) acquired in the presence (A) and in absence (B) of 16-doxylstearic acid is reported. Ala 30, Ile 31, and Gly 33 are drastically affected by a spin label effect with a significant decrease of the Hα-NH signals. Figure 2 shows the best NMR structure obtained in SDS, selected on the basis of the target function value; the side chains of the residues affected by the 16-doxylstearic acid are displayed. This result provides evidence that the C-terminal portion of Aβ-(25−35), arranged in an α-helical structure, is deeply embedded in the SDS micelle.

2. HFIP Analysis. 2.1. CD Spectroscopy. The conformational preferences of Aβ-(25−35) were determined from the CD spectra acquired in mixtures of water/HFIP with different ratios (v/v). The spectra corresponding to 20%, 30%, and 40% of HFIP in water have the typical shape of random coil structures, while a significant change in the spectrum intensity is evident starting from 50/50 HFIP/water composition. The CD curves corresponding to mixtures 50/50, 60/40, and 70/30 HFIP/water are typical of turn−helical structures.

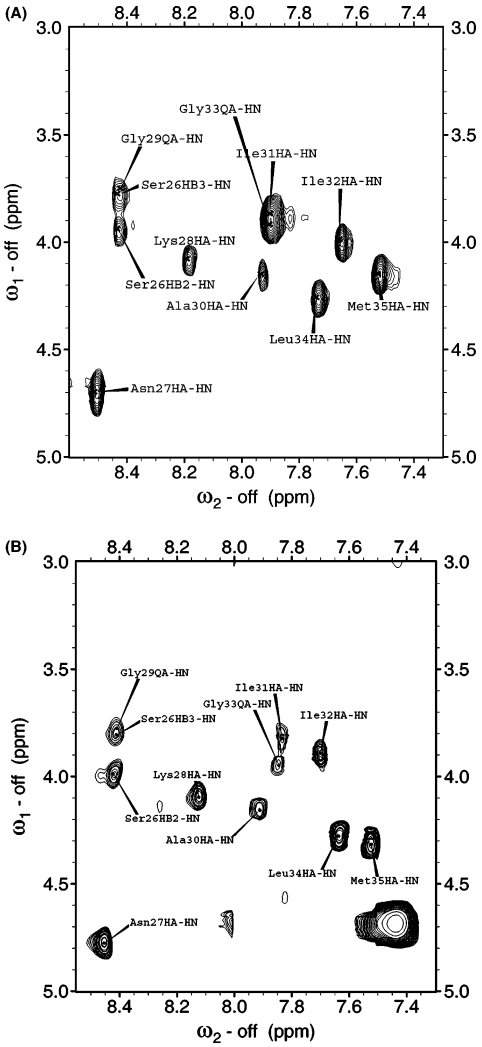

Figure 1. Fingerprint region of the 600 MHz TOCSY spectra of Aβ-(25−35) recorded in 100 mM SDS water solution at 300 K (A) and upon addition of 5-doxylstearic acid at a concentration of one spin label per micelle (B).

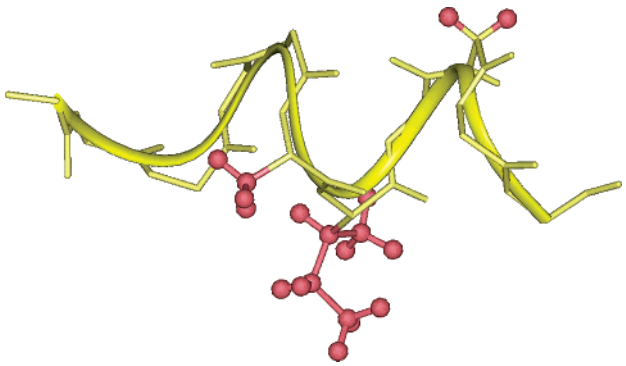

Figure 2. NMR structure of Aβ-(25−35) in 100 mM SDS aqueous solution. The structure was derived from DYANA calculations and was chosen according to the lowest value of the target function. The residues affected by paramagnetic spins are in red and highlighted with ball-and-stick rendering.

The helix content, as estimated by standard linear combination fits of the spectra,[28] increases almost linearly from 17% in neat water to about 80% in HFIP/water 80/20 (v/v), i.e., reaching a value very similar to that of Aβ-(1−42) under the same experimental conditions.[12] A comparison of the CD spectra recorded in some of the mixtures tested is shown in Figure 3. In the selected mixtures, the CD spectra are essentially unchanged in the temperature range 10−45 °C (data not shown), suggesting a high conformational stability of Aβ-(25−35) in these solvent media. Moreover, the Aβ-(25−35) solutions in aqueous HFIP were very stable because there was no evidence of aggregation or precipitation and the NMR spectra did not change over several weeks.

On the basis of these results, we performed an NMR investigation of Aβ-(25−35) in the presence of a low (HFIP/water 20/80) and a high (HFIP/water 80/20) amount of HFIP. The two mixtures are representative of a mainly aqueous medium and of a mainly apolar environment, respectively. Furthermore, the NMR data of Aβ-(25−35) in HFIP/water 80/20 allows a comparison with the NMR structure of Aβ-(1−42), which has been recently determined by us in the same solvent mixture.[12]

2.2. NMR Spectrometry. A whole set of 1D and 2D protonic spectra were recorded in 20/80 and 80/20 HFIP/water mixtures. Also, under these experimental conditions, no significant changes were observed in the concentration range of 0.5−15 mM, showing the absence of aggregated forms. The assignment of the proton resonances of Aβ-(25−35) was achieved by following the same procedure reported above.

In Figure 4 all short- and medium-range NOE effects involving the backbone protons of Aβ-(25−35) in both the HFIP/water mixtures are summarized.

The inspection of the bar diagram corresponding to the 20/80 HFIP/water mixture shows a low number of diagnostic (i, $i + 2$) and (i, $i + 3$) effects. Moreover, all of them are located in the N-terminal segment 25−29, while the C-terminal region of the peptide is characterized by disordered structures. In contrast, a more regular pattern was found in the bar diagram corresponding to the 80/20 HFIP/water mixture, where sequential NH_i-NH_{i+1} NOEs and diagnostically critical (i, $i + 2$) and (i, $i + 3$) effects encompassing residues 28−34 are present. The data are consistent with the presence of a well-defined α-helical structure in the C-terminal region. A less regular pattern consistent with the presence of partially folded structures was observed for the N-terminal segment.

2.3. Structure Calculation. The same calculation procedure followed in SDS experiments was adopted. Among 50 calculated structures the resulting best 20 were selected according to the lowest values of their target function. They were subjected to further procedures of minimization with the SANDER module of the AMBER 5.0 software[29,30] using the DYANA derived restraints.

The model of Aβ-(25−35) calculated on the basis of NOE data in the 20/80 HFIP/water mixture shows the prevalence of disordered structures particularly in the C-terminal region, whereas a significant presence of ordered conformations is detectable at level of the N-terminal residues. The conformers of the N-terminal segment of Aβ-(25−35) in 20/80 HFIP/water are well fitted (the rmsd for the backbone between residues 25 and 28 is 0.46 Å) (Figure 5). The PDB files subjected to the PROMOTIF software[31] for the validation of the structural results show the presence of a type I β-turn

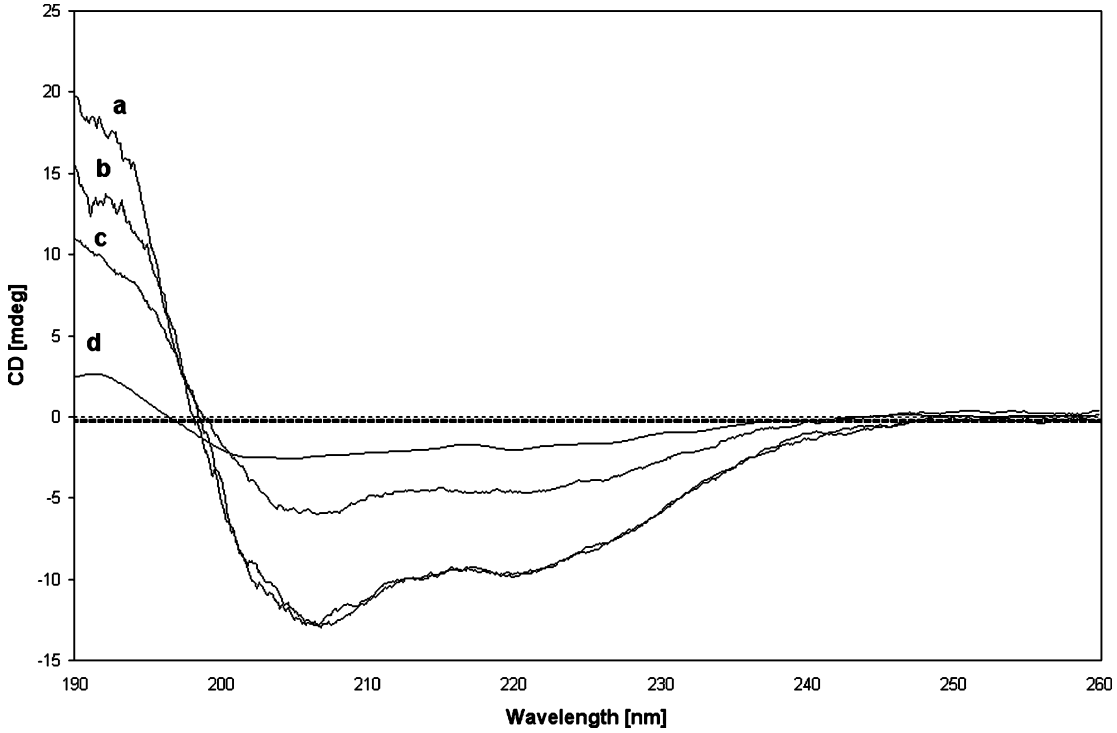

Figure 3. Circular dichroism curves of Aβ-(25−35) at different HFIP/water compositions. The spectra were recorded at room temperature at 80/20 (a), 70/30 (b), 30/70(c), and 20/80 (d) (v/v) HFIP/water composition. Total molar ellipticities are reported vs wavelength in nm.

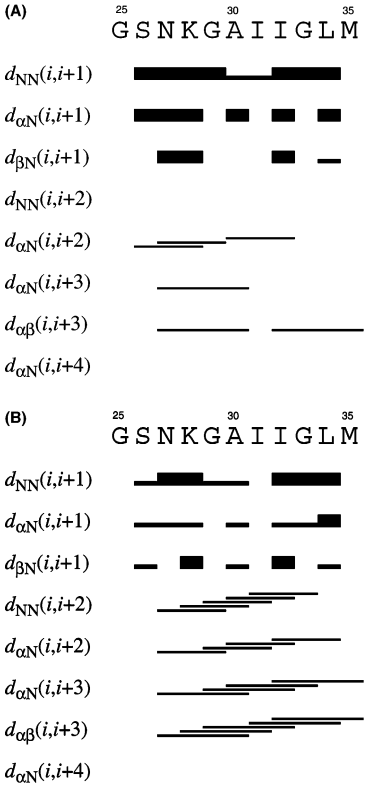

Figure 4. Sequential and medium-range NOEs for Aβ-(25−35). Data were obtained from a 600 MHz NOESY experiment with a mixing time of 150 ms and collected in HFIP/water 20/80 v/v (A) and HFIP/water 80/20 (B) at 300 K.

centered on residues 26 and 27. Unconstrained minimization of the structures did not produce any major rearrangement in this region, which instead would be expected if the observed dihedrals were imposed by the influence of artifactual NMR restraints.

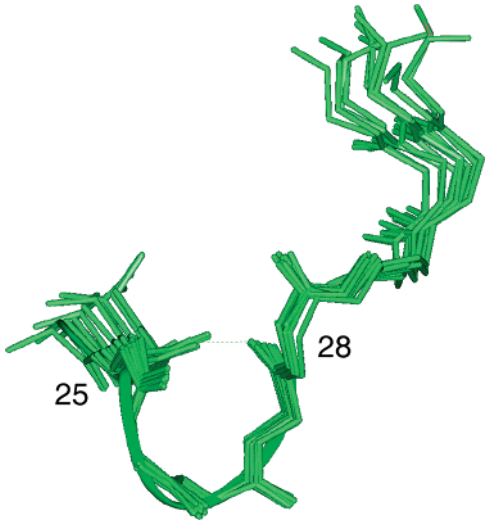

Figure 5. The best 20 calculated structures of Aβ-(25−35) in HFIP/water 20/80 as derived from DYANA calculations and energy-minimized using the SANDER module of the AMBER 5.0 software. The structures are fitted on the heavy backbone atoms of the 25−28 segment.

Figure 6 reports the overlap of the best 20 NMR structures of Aβ-(25−35) calculated from NMR data of HFIP/water 80/20. The models are fitted at the level of the residues 28−34, where Aβ-(25−35) is characterized by the presence of a helical structure (rmsd for the backbone is 0.68 Å). As expected from the NOE data, a significant decrease of structural regularity is observable in the N-terminal segment. Notwithstanding, a careful glance toward the dihedral angles relative to the 26−28 residues shows that they are generally compatible with the presence of a turn structure. The dihedral angles relative to the structures calculated in the two HFIP/water mixtures are reported in Table 1.

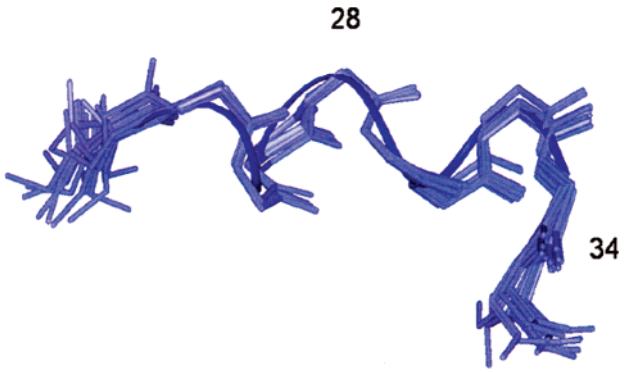

Figure 6. The best 20 calculated structures of Aβ-(25−35) in HFIP/water 80/20 as derived from DYANA calculations and energy-minimized using the SANDER module of the AMBER 5.0 software. The structures are fitted on the heavy backbone atoms of the 28−34 segment.

Table 1. Values of the ϕ and ψ Dihedral Angles of Aβ-(25−35) Structures Derived from NMR Data in HFIP/Water (20/80 and 80/20 v/v) at 600 MHz and 300 K

	HFIP/water 20/80		HFIP/water 80/20	
residue	ϕ (deg)	ψ (deg)	ϕ (deg)	ψ (deg)
Gly^{25}		−99.0 ± 33		−169.3 ± 35
Ser^{26}	−88.8 ± 49	−35.9 ± 38	−74.5 ± 26	−151.6 ± 34
Asn^{27}	−107.8 ± 30	−15.4 ± 25	−60.9 ± 15	−15.7 ± 22
Lys^{28}	−92 ± 34	−42.1 ± 16	−5.3 ± 14	−40.3 ± 15
Gly^{29}	53.1 ± 27	−18.9 ± 14	−55.8 ± 13	−17.4 ± 16
Ala^{30}	−76.2 ± 19	−120.5 ± 13	−103.4 ± 12	−26.4 ± 14
Ile^{31}	−37.8 ± 16	−49.5 ± 12	−47.7 ± 12	−24.8 ± 20
Ile^{32}	−85.8 ± 12	−135.1 ± 15	−51.1 ± 13	−23.8 ± 16
Gly^{33}	111.0 ± 13	−50.2 ± 14	−67.5 ± 15	−4± 13
Leu^{34}	46.0 ± 18	−79.5 ± 23	170.7 ± 19	48.2 ± 12
Met^{35}	−75.2 ± 22		−41.6 ± 19	

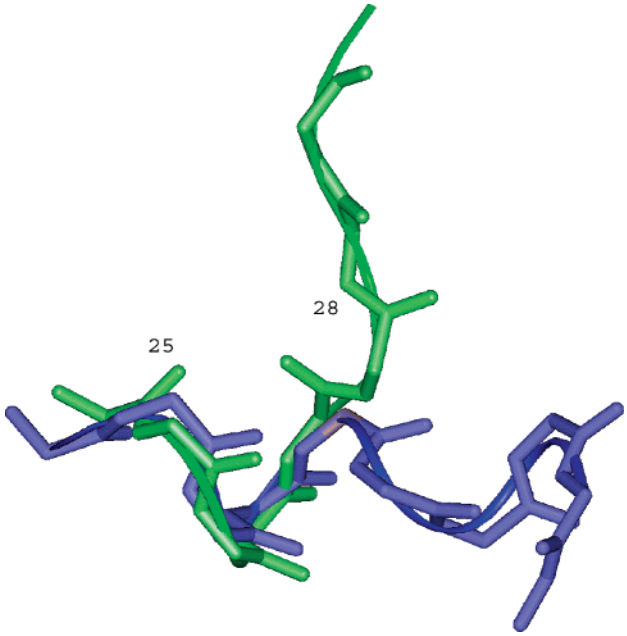

Figure 7. Overlapping of the best NMR structures of Aβ-(25−35) in HFIP/water 80/20 (blue) and HFIP/water 20/80 (green) mixtures.

In Figure 7 a comparison of the best NMR structures of Aβ-(25−35) in the two solvent mixtures is displayed. It is evident that there is a significant degree of similarity in the N-terminal residues, where the presence of a turn conformation is conserved.

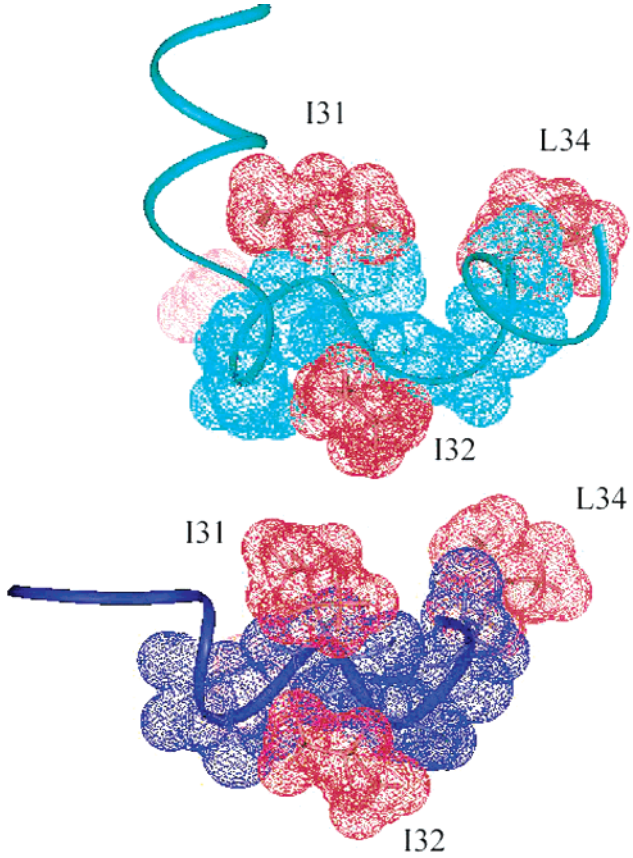

Figure 8. Structural comparison of the surfaces relative to the NMR structure of Aβ-(25−35) in HFIP/water 80/20 (blue) and Aβ-(1−42) (cyan) in HFIP/water 80/20. The surfaces are colored according to the hydrophobicity scale where the hydrophobic residues are in red and the hydrophilic residues are in blue.

2.4. Aβ-(25−35) and Aβ-(1−42) Structure Comparison. Recently we have determined the NMR structure of Aβ-(1−42) in aqueous HFIP.[12] In this environment the amyloid peptide shows two helical stretches connected by a kink region centered on a regular type I β-turn involving the residues 25−28. The same structural motif has been found in Aβ-(25−35) in the explored fluorinated mixtures. Moreover, depending on the experimental conditions, a helical stretch spanning residues 28−34 has been found in full-length Aβ as well as in Aβ-(25−35). Finally, Figure 8 shows that the molecular surfaces of Aβ-(1−42) and Aβ-(25−35) in HIFP 80/20 are very similar, showing a common orientation of the hydrophobic side chains in the more significantly ordered region.

Discussion

The fight against the Alzheimer disease is an important challenge in pharmaceutical research because of the increasing incidence of this pathology correlated to the life elongation.

The design of molecules able to interact with the amyloid peptides as inhibitors of fibril formation or as inhibitors of amyloid membrane pore formation constitutes a basic approach in the development of anti-Alzheimer therapies. Despite the large amount of experimental data, it is not clear whether the fibrils of amyloid peptides are the cause of Alzheimer pathology or if alternatively they have a protective function, while

the pathological cause is the amyloid membrane disruption activity. In both the cases the study of the conformational properties of Aβ peptides is the basis for the design of molecules with "anti-amyloid" activity.

The difficulty of manipulating the natural proteins to test their structural properties has prompted the scientific community to devise suitable models sharing with natural proteins the in vitro amyloidogenic property. Similar to Aβ-(1−42), Aβ-(25−35) may assume different conformations in vitro, depending on the experimental conditions. However, a reduced size and a higher solubility allow for a better biophysical characterization that might help to dissect the contribution of single interactions as hydrophobic, electrostatic, or hydrogen bonds in the different conformational states.

In the present study we have determined the high-resolution solution structure of the Aβ-(25−35) under different experimental conditions by 2D NMR spectrometry. The comparison among the structures obtained might help unveil the regions that are mainly affected by the environmental conditions.

The SDS micellar solution defines a nonisotropic apolar environment where the membrane interaction activities of the biomolecules can be tested. The solution structure of Aβ-(25−35) in SDS confirmed the presence of a helical stretch encompassing residues 28−34, already reported in LiDS micelles;[16] the region 25−27 characterized by a low number and poor quality of NOE data appears less ordered in this medium. A comparison of our SDS structure with the corresponding region of the full length Aβ-(1−40)[32] and Aβ-(1−42)[33] in SDS micelles shows that Aβ-(25−35) retains the structural features of its parent peptide Aβ-(1−42) in similar environments. The NMR analysis in the presence of spin labels allows the definition of the orientation of Aβ-(25−35) with respect to the micelles as a model of the orientation with respect to the cell membrane. Indeed, the perturbation of chemical shifts and intensities of the signals in the presence of 16-doxylstearic acid shows that only the C-terminal part of Aβ-(25−35) is inserted into SDS micelles. These results suggest a natural propensity of the C-terminal region, which shows the typical amino acid composition of a transmembrane helix,[34] to interact with an apolar environment. Moreover, the resemblance to the solution structure of Aβ-(1−40)[32] and Aβ-(1−42)[33] in SDS supports the hypothesis of a similar orientation of the full-length Aβ with respect to the cell membrane.

In the search for experimental conditions that may favor the monitoring of different conformational states using different polarity conditions, we resorted to HFIP/water mixtures with different composition. These have been proved, in the 80/20 HFIP/water composition, to produce a completely stable, ordered solution of Aβ-(1−40)[19] and Aβ-(1−42).[12] In contrast, the HFIP/water mixtures with a content of water higher than 20% produce insoluble aggregates. Thus, the observation of the conformational properties of Aβ-(25−35) in mixtures with different HFIP/water composition was performed to monitor the conformational behavior of Aβ-(25−35) in media with different polarity. The CD data recorded in HFIP/water mixtures from 80/20 v/v HFIP/water to 20/80 v/v HFIP/water show that an amount of water greater than 50% produces a drastic modification of the peptide folding. To follow the conformational modifications derived from increasing medium polarity, we have selected two extreme conditions: a 20/80 HFIP/water mixture, which may resemble the aqueous interface between the membrane surface and the extracellular medium, and a 80/20 HFIP/water mixture with a higher apolar character to simulate the lipid environment. Interestingly, the structure of Aβ-(25−35) in the 80/20 HFIP/water mixture is characterized by a high degree of ordered, folded conformation particularly in the C-terminal portion that is almost identical to the one previously discussed in SDS. In comparison, the N terminus appears to be less ordered with a slight presence of conformers characterized by a β-turn in the 25−27 region. The structural similarity between Aβ-(1−42) and Aβ-(25−35) in HFIP/water 80/20 suggests a common neurotoxic mechanism possibly based on the formation of ion channels into the membrane.[35] Interestingly the conformational peculiarities of Aβ-(25−35) in the HFIP/water 80/20 apolar environment further support the recent hypothesis that amyloid peptides can enhance the association of liposomes with cells, producing an enhancement of viral infection.[13] This result gives further relevance to the previously highlighted analogies between the fusion domain of the influenza virus haemagglutinin,[36] several membrane interacting peptides,[37] and Aβ-peptides.

The solution structure of Aβ-(25−35) in an inverted HFIP/water ratio (20/80 v/v) is characterized by a decrease of regular folding in the C-terminal region, while a significant regularity in the structure is conserved only in the 25−28 segment, characterized by a β-turn structure. The structural peculiarity of this region emphasizes the role of the kink conformation encompassing residues 25−27 that appears to be a general feature of amyloid peptides in all the solution conditions explored as well as in the crystal state. This region in the full-length Aβ corresponds to a kink connecting two helical stretches[12,32,33] and has a similar arrangement also in the model of fibrillar Aβ-(1−40) reported very recently.[38]

A possible biological role of this region is suggested by the observation that the mutant of Aβ-(25−35) in which the Asn 27 has been replaced with Ala loses the neurotoxicity.[16] The solution structure of this peptide is very similar to that of the parent Aβ-(25−35) but for the mutated residue, which is also included in the N-terminal α-helix. The different structures of Aβ-(25−35) in HFIP/water mixtures give experimental evidence of the propensity of the peptide to lose the structural regularity at a particular point of the sequence as a function of the environment, behaving as a partially unfolded intermediate in the aggregation process.

Experimental Section

Solid-Phase Peptide Synthesis and Purification. Aβ-(25−35) was synthesized according to published methods using standard solid-phase synthesis techniques[39] with a Milligen 9050 synthesizer. Protected amino acids and chemicals were purchased from Bachem, Novabiochem, or Fluka (Switzerland). The resin loaded with methionine on the poly(ethylene glycol)/polystyrene support (Fmoc-Met-PEG-PS) was from Millipore (Waltham, MA). N^{α}-Fmoc derivatives of amino acids were used in the coupling reactions, and all lateral amino acid protections were trifluoroacetic acid labile.

Table 2. Analytical Properties of Aβ-(25−35) Peptide

sequence	purity (%)	t_R [a] (min) I	t_R [a] (min) II	MH^+ [b] calculated	MH^+ [b] found
H-Gly-Ser-Asn-Lys-Gly-Ala-Ile-Ile-Gly-Leu-Met-OH	>98	13.37	10.93	1061.3	1061.2

[a] t_R is the retention time determined by analytical HPLC. [b] The mass ion (MH^+) was obtained from MALDI-TOF mass spectrometry.

Fmoc-Met-PEG-PS resin (0.21 mequiv/g, 0.5 g) was treated with piperidine (20%) in DMF, and the N^{α}-Fmoc amino acid derivatives (4-fold excess) were sequentially coupled to the growing peptide chain by using *O*-(7-azabenzotriazol-1-yl)-1,1,3,3-tetramethyluronium hexafluorophosphate (HATU)[40] (4-fold excess) in DMF, and the coupling reaction time was 1 h.

Double coupling was required in the acylation step of Leu and Ile. Piperidine (20%) in DMF was used to remove the Fmoc group at all steps. After deprotection of the last N^{α}-Fmoc group, the peptide resin was washed with methanol and dried in vacuo to yield the protected peptide-PEG-PS−resin. The protected peptide was cleaved from the resin by treatment with TFA/H_2O/phenol/ethanedithiol/thioanisole (reagent K) (82.5:5:5:2.5:5 v/v) 10 mL/0.5 g of resin at room temperature for 1 h.[41] After filtration of the exhausted resin, the solvent was concentrated in vacuo and the residue was triturated with ether.

The crude peptide was purified by preparative reversed-phase HPLC using a Water Delta Prep 4000 system with a Waters PrepLC 40 mm assembly column C18 (30 cm × 4 cm, 300 Å, 15 mm spherical particle size column). The column was perfused at a flow rate of 40 mL/min with a mobile phase containing solvent A (water in 0.1% TFA), and a linear gradient from 5% to 30% of solvent B (acetonitrile in 0.1% TFA) in 25 min was adopted for the elution of the peptide. The pure fraction was collected to yield a white powder after lyophilization.

HPLC analyses were performed on a Beckman 125 liquid chromatography fitted with an Alltech column C18 (4.6 mm × 150 mm, 5 mm particle size) and equipped with a Beckman 168 diode array detector, using the above solvent system (solvents A and B) programmed at a flow rate of 1 mL/min with a linear gradient (I) from 0% to 25% or (II) from 0% to 40% B in 25 min. The molecular weight of the compound was determined by a MALDI-TOF (matrix-assisted laser desorption ionization time-of-flight) analysis using a Hewlett-Packard G2025A LD-TOF mass spectrometer and α-cyano-4-hydroxycinnamic acid as a matrix. The analytical properties of Aβ-(25−35) peptide are reported in Table 2.

Circular Dichroism. All CD spectra were recorded using a JASCO J-810 spectropolarimeter with a cell of 1.0 mm path length. CD measurements were performed at 298 K, using a range from 260 to 190 nm, 1 nm bandwidth, 4 accumulations, and 10 nm/min of scanning speed. The SDS sample was obtained by dissolving the peptide in an aqueous solution of 100 mM SDS at pH 4.15. Water/HFIP samples were prepared by dissolution of Aβ-(25−35) in water/HFIP mixtures (composition 20/80, 30/70, 40/60, 50/50, 60/40, 70/30 by volume). The concentration of the peptide in these solutions was 0.1 mM. For estimation of secondary structure content, CD spectra were analyzed by a linear combination fit using the reference data of Greenfield and Fasman.[42]

NMR Spectrometry. The samples for NMR spectroscopy were prepared by dissolving the appropriate amount of Aβ-(25−35) in 0.5 mL of solution to obtain a concentration 1.0 mM of peptide. For SDS measurements, the concentration of deuterated SDS-d_{25} was 100 mM. Assuming an SDS micelle aggregation number of 56, this corresponds to a micelle concentration of 1.8 mM. The H_2O/D_2O ratio was 90/10.[43] For spin label experiments, the 5- and 16-doxylstearic acids were solubilized in methanol-d_4 and then added to the samples.

The composition of the water/HFIP mixtures for NMR measurements was respectively 20/80 and 80/20 v/v. The concentration of the peptide in these solutions was 1.0 mM.

NMR spectra were recorded on a Bruker DRX-600 spectrometer. One-dimensional (1D) NMR spectra were recorded in the Fourier mode with quadrature detection, and the water signal was suppressed by low-power selective irradiation in the homogated mode. DQF-COSY, TOCSY, and NOESY[21−23] experiments were run in the phase-sensitive mode using quadrature detection in ω_1 by time-proportional phase increase of the initial pulse. Data block sizes were 2048 addresses in t_2 and 512 equidistant t_1 values. Before Fourier transformation, the time domain data matrices were multiplied by shifted $\sin^2$ functions in both dimensions. A mixing time of 70 ms was used for the TOCSY experiments. NOESY experiments were run at 300 K with mixing times in the range of 100−250 ms. The qualitative and quantitative analysis of DQF-COSY, TOCSY, and NOESY spectra was achieved using the SPARKY software.[24]

Molecular Modeling. Peak volumes were translated into upper distance bounds with the routine CALIBA of the DYANA software.[25]

The necessary pseudoatom corrections were applied for nonstereospecifically assigned protons at prochiral centers and for the methyl group of aliphatic side chains. After the redundant and duplicated constraints were discarded, the final list for the structure of Aβ(25−35) in HFIP/water included 78 intraresidue constraints and 33 interresidue constraints, which were used to generate an ensemble of 100 structures by the standard protocol of simulated annealing in torsion angle space implemented in DYANA (using 6000 steps). No dihedral angle restraints and no hydrogen bond restraints were applied. The best 20 structures, which had low values of the target functions (0.83−1.19) were refined by in vacuo minimization in the AMBER 1991 force field, using the program SANDER of the AMBER 5.0 suite.[30]

To mimic the effect of solvent screening, all net charges were reduced to 20% of their real value, and moreover, a distance-dependent dielectric constant ($\epsilon = r$) was used. The cutoff for nonbonded interactions was 12 Å. The NMR-derived upper bounds were imposed as semiparabolic penalty functions, with force constants of 16 kcal mol^{-1} $Å^{-2}$; the function was shifted to linearity when the violation exceeded 0.5 Å. The best 10 structures after minimization had AMBER energies ranging from −441.4 to −391.1 kcal/mol. The final structures were analyzed using the Insight 98.0 program.[44] Computations were performed on SGI Indigo II computers.

Coordinates. Coordinates have been deposited in the Protein Data Bank. The access codes are 1QXC and 1QWP for Aβ-(25−35) in HFIP/water 20/80 and HFIP/water 80/20 mixtures, respectively. The access code is 1QYT for Aβ-(25−35) in 100 mM SDS aqueous solution.

Acknowledgment. We are very grateful to Professor P. A. Temussi for useful and stimulating discussions. We thank Professor Kanfer for critical reading of the manuscript. This work was supported by grants from Regione Campania (legge regionale 41/94), Italy and Progetto Strategico Alzheimer, Ministero della Salute-Regione Lazio, Italy.

Appendix

Abbreviations. Abbreviations used for amino acids and designation of peptides follow the rules of the IUPAC-IUB Commission of Biochemical Nomenclature in *J. Biol. Chem.* **1972**, *247*, 977−983. Amino acid symbols denote L-configuration unless otherwise indicated. In addition, the following additional abbreviations are used: AD, Alzheimer disease; SDS, sodium dodecyl sulfate; CNS, central nervous system; SAR, structure−

activity relationship; NMR, nuclear magnetic resonance; CD, circular dichroism; Fmoc, 9-fluorenylmethoxycarbonyl; HPLC, high-performance liquid chromatography; HFA, 1,1,1,3,3,3,-hexafluoroacetone; DQF-COSY, double quantum filtered correlated spectroscopy; TOCSY, total correlated spectroscopy; NOESY, nuclear Overhauser enhancement spectroscopy; NOE, nuclear Overhauser effect; MD, molecular dynamics; 1D, 2D, and 3D, one-, two-, and three-dimensional; TFA, trifluoracetic acid; HFIP, hexafluoroisopropanol.

References

(1) Sunde, M.; Blake, C. From the globular to the fibrous state: protein structure and structural conversion in amyloid formation. *Q. Rev. Biophys.* **1998**, *31*, 1−39.

(2) Rochet, J. C.; Lansbury, P. T., Jr. Amyloid fibrillogenesis: themes and variations. *Curr. Opin. Struct. Biol.* **2000**, *10*, 60−68.

(3) Sipe, J. D.; Cohen, A. S. Review: history of the amyloid fibril. *J. Struct. Biol.* **2000**, *130*, 88−98.

(4) Kirschner, D. A.; Abraham, C.; Selkoe, D. J. X-ray diffraction from intraneuronal paired helical filaments and extraneuronal amyloid fibers in Alzheimer disease indicates cross-β conformation. *Proc. Natl. Acad. Sci. U.S.A.* **1986**, *83*, 503−507.

(5) Glenner, G. G.; Wong, C. W. Alzheimer's disease and Down's syndrome: sharing of a unique cerebrovascular amyloid fibril protein. *Biochem. Biophys. Res. Commun.* **1984**, *120*, 885−890.

(6) Selkoe, D. J. Translating cell biology into therapeutic advances in Alzheimer's disease. *Nature* **1999**, *399* (Suppl.), A23−A31.

(7) Selkoe, D. J. Amyloid β-protein and the genetics of Alzheimer's disease. *J. Biol. Chem.* **1996**, *271*, 18295−18298.

(8) Temussi, P. A.; Masino, L.; Pastore, A. From Alzheimer to Huntington: why is a structural understanding so difficult? *EMBO J.* **2003**, *22*, 355−361.

(9) Terry, R. D. The neuropathology of Alzheimer disease and the structural basis of its cognitive alterations. In *Alzheimer Disease*; Terry, R. D., Katzman, R., Bick, K. L., Sisodia, S. S., Eds.; Lippincott Williams and Wilkins: Philadelphia, PA, 1999; pp 187−206.

(10) Lambert, M. P.; Barlow, A. K.; Chromy, B. A.; Edwards, C.; Freed, R.; Liosatos, M.; Morgan, T. E.; Rozovsky, I.; Trommer, B.; Viola, K. L.; Wals, P.; Zhang, C.; Finch, C. E.; Krafft, G. A.; Klein, W. L. Diffusible, nonfibrillar ligands derived from Aβ1−42 are potent central nervous system neurotoxins. *Proc. Natl. Acad. Sci. U.S.A.* **1998**, *95*, 6448−6453.

(11) Harper, J. D.; Wong, S. S.; Lieber, C. M.; Lansbury, P. T. Assembly of Aβ amyloid protofibrils: an in vitro model for a possible early event in Alzheimer's disease. *Biochemistry* **1999**, *38*, 8972−8980.

(12) Crescenzi, O.; Tomaselli, S.; Guerrini, R.; Salvadori, S.; D'Ursi, A. M.; Temussi, P. A.; Picone, D. Solution structure of the Alzheimer amyloid β-peptide (1−42) in an apolar microenvironment. Similarity with a virus fusion domain. *Eur. J. Biochem* **2002**, *269*, 5642−5648.

(13) Wojtowicz, W. M.; Farzan, M.; Joyal, J. L.; Carter, K.; Babcock, G. J.; Israel, D. I.; Sodroski, J.; Mirzabekov, T. Stimulation of enveloped virus infection by β-amyloid fibrils. *J. Biol. Chem.* **2002**, *277*, 35019−35024.

(14) Pike, C. J.; Walencewicz-Wasserman, A. J.; Kosmoski, J.; Cribbs, D. H.; Glabe, C. G.; Cotman, C. W. Structure−activity analyses of β-amyloid peptides: contributions of the β 25−35 region to aggregation and neurotoxicity. *J. Neurochem.* **1995**, *64*, 253−265.

(15) Terzi, E.; Holzemann, G.; Seelig, J. Alzheimer β-amyloid peptide 25−35: electrostatic interactions with phospholipid membranes. *Biochemistry* **1994**, *33*, 7434−7441.

(16) Kohno, T.; Kobayashi, K.; Maeda, T.; Sato, K.; Takashima, A. Three-dimensional structures of the amyloid β-peptide (25−35) in membrane-mimicking environment. *Biochemistry* **1996**, *35*, 16094−16104.

(17) Del Mar Martinez-Senac, M.; Villalain, J.; Gomez-Fernandez, J. C. Structure of the Alzheimer β-amyloid peptide (25−35) and its interaction with negatively charged phospholipid vesicles. *Eur. J. Biochem.* **1999**, *265*, 744−753.

(18) Rajan, R.; Awasthi, S. K.; Bhattachajya, S.; Balaram, P. Teflon-coated peptides: hexafluoroacetone trihydrate as a structure stabilizer for peptides. *Biopolymers* **1997**, *42*, 125−128.

(19) Vieira, E. P.; Hermel, H.; Möhwald, H. Change and stabilization of the amyloid-β (1−40) secondary structure by fluorocompounds. *Biochim. Biophys. Acta* **2003**, *1645*, 6−14.

(20) Wüthrich, K. *NMR of Proteins and Nucleic Acids*; John Wiley & Sons: New York, 1986.

(21) Piantini, U.; Soerensen, O. W.; Ernst, R. R. Multiple quantum filters for elucidating NMR coupling networks. *J. Am. Chem. Soc.* **1982**, *104*, 6800−6801.

(22) Bax, A.; Davis, D. G. Mlev-17-based two-dimensional homonuclear magnetization transfer spectroscopy. *J. Magn. Reson.* **1985**, *65*, 335−360.

(23) Jeener, J.; Meyer, B. H.; Bachman, P.; Ernst, R. R. Investigation of exchange processes by two-dimensional NMR spectroscopy. *J. Chem. Phys.* **1979**, *71*, 4546−4553.

(24) Goddard, T. D.; Kneller, D. G. SPARKY 3, University of California, San Francisco.

(25) Guntert, P.; Mumenthaler, C.; Wüthrich, K. Torsion angle dynamics for NMR structure calculation with the new program DYANA. *J. Mol. Biol.* **1997**, *273*, 283−298.

(26) Jarvet, J.; Zdunek, J.; Damberg, P.; Graslund, A. Three-dimensional structure and position of porcine motilin in sodium dodecyl sulfate micelles determined by ^{1}H NMR. *Biochemistry* **1997**, *36*, 8153−8163.

(27) Lindberg, M.; Jarvet, J.; Langel, U.; Graslund, A. Secondary structure and position of the cell-penetrating peptide transportan in SDS micelles as determined by NMR. *Biochemistry* **2001**, *40*, 3141−3149.

(28) Johnson, W. C., Jr. Protein secondary structure and circular dichroism: a practical guide. *Proteins* **1990**, *7*, 205−214.

(29) Weiner, S. J.; Kollman, P. A.; Case, D. A.; Singh, U. C.; Chio, C.; Alagona, G.; Profeta, S.; Weiner, P. A new force field for molecular mechanical simulation of nucleic acids and proteins. *J. Am. Chem. Soc.* **1984**, *106*, 765−784.

(30) Case, D. A.; Pearlman, D. A.; Caldwell, J. W.; Cheatham, T. E., III; Ross, W. S.; Simmerling, C. L.; Darden, T. A.; Merz, K. M.; Stanton, R. V.; Cheng, A. L.; Vincent, J. J.; Crowley, M.; Ferguson, D. M.; Radmer, R. J.; Seibel, G. L.; Singh, U. C.; Weiner, P. K.; Kollman, P. A. *AMBER 5*; University of California, San Francisco, 1997.

(31) Hutchinson, E. G.; Thornton, J. M. PROMOTIF−a program to identify and analyze structural motifs in proteins. *Protein Sci.* **1996**, *2*, 212−220.

(32) Coles, M.; Bicknell, W.; Watson, A. A.; Fairlie, D. P.; Craik, D. J. Solution structure of amyloid β-peptide(1−40) in a water−micelle environment. Is the membrane-spanning domain where we think it is? *Biochemistry* **1998**, *37*, 11064−11077.

(33) Shao, H.; Jao, S.; Ma, K.; Zagorski, M. G. Solution structures of micelle-bound amyloid β-(1−40) and β-(1−42) peptides of Alzheimer's disease. *J. Mol. Biol.* **1999**, *285*, 755−773.

(34) Eilers, M.; Shekar, S. C.; Shieh, T.; Smith, S. O.; Fleming, P. J. Internal packing of helical membrane proteins. *Proc. Natl. Acad. Sci. U.S.A.* **2000**, *97*, 5796−5801.

(35) Rhee, S. K.; Quist, A. P.; Lal, R. Amyloid β-protein-(1−42) forms calcium-permeable, Zn^{2+}-sensitive channel. *J. Biol. Chem.* **1998**, *273*, 13379−13382.

(36) Han, X.; Bushweller, J. H.; Cafiso, D. S.; Tamm, L. K. Membrane structure and fusion-triggering conformational change of the fusion domain from influenza hemagglutinin. *Nat. Struct. Biol.* **2001**, *8*, 715−720.

(37) Hristova, K.; Dempsey, C. E.; White, S. H. Structure, location, and lipid perturbations of melittin at the membrane interface. *Biophys. J.* **2001**, *80*, 801−811.

(38) Petkova, A. T.; Ishii, Y.; Balbach, J. J.; Antzutkin, O. N.; Leapman, R. D.; Delaglio, F.; Tycko, R. A structural model for Alzheimer's β-amyloid fibrils based on experimental constraints from solid state NMR. *Proc. Natl. Acad. Sci. U.S.A.* **2002**, *99*, 16742−16747.

(39) Atherton, E.; Sheppard, R. C. In *Solid Phase Peptide Synthesis*; Rickwood, D., Hames, B. D., Eds.; IRL Press: Oxford, U.K., 1989.

(40) Carpino, L. A. 1-Hydroxy-7-azabenzotriazole. An efficient peptide coupling additive. *J. Am. Chem. Soc.* **1993**, *115*, 4397−4398.

(41) King, D. S.; Fields, C. G.; Fields, G. B. A cleavage method which minimizes side reactions following Fmoc solid phase peptide synthesis. *Int. J. Pept. Protein Res.* **1990**, *36*, 255−266.

(42) Greenfield, N.; Fasman, G. D. Computed circular dichroism spectra for the evaluation of protein conformation. *Biochemistry* **1969**, *8*, 4108−4116.

(43) Lauterwein, J.; Bosch, C.; Brown, L. R.; Wuthrich, K. Physicochemical studies of the protein−lipid interactions in melittin-containing micelles. *Biochim. Biophys. Acta* **1979**, *556*, 244−264.

(44) MSI Molecular Simulations, 965 Scranton Road, San Diego, CA 92121-3752.

JM040773O